Aromatic C–C Bond Cleavage in a Curved π-System of Amino-corannulene

Weijie Guo+, Wanjian Ding+, Yuqing Yao, Suchada Rajca, Qiaolian Li, Hua Jiang*, Andrzej Rajca*, and Ying Wang*

Supporting Information Placeholder

ABSTRACT: We report a metal- and oxidant-free aromatic C–C bond cleavage in the curved corannulene skeleton. Reaction of 1-aminocorannulene with hydrazonyl chloride generates an amidrazone intermediate that undergoes facile intramolecular proton migrations and ring-annulation to give 1,2,4-triazole derivative of planar benzo[*ghi*]fluoranthene, in which the release of strain associated with the curved π-surface and the formation of aromatic triazole moiety are the driving forces. This report provides new insights into the aromatic C–C bond cleavage.

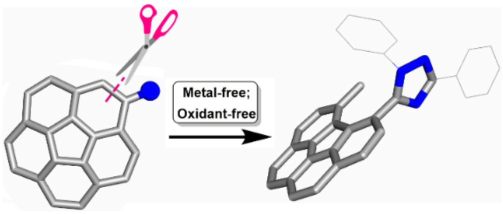

Selective cleavage of C–H and C–C bonds provide powerful strategies to efficiently edit organic molecules. Among all types of C–H[1,2] and C–C[2–11] bond activations, the selective cleavage of aromatic C–C bonds poses undoubtedly the greatest synthetic challenge due to the aromaticity (to give a very high C–C bond dissociation energy; e.g., 114 kcal mol^{-1} in benzene).[12] To date, aromatic C–C bond cleavage is still a largely unexplored research area, with a small number of literature precedence concerning mainly the metal- and the oxidant/oxygenase-mediated reactions.[5–11] The metal-mediated aromatic C–C cleavages typically use directing groups to facilitate thermodynamically favourable interactions of metals with aromatic C–C bonds, to induce direct metal insertions[13–16] or ring contractions[17–19]/expansions[20] that create ring strains, leading to the C–C bond scissions occurring typically under harsh reaction condition. On the other hand, the C–C bond cleavage reactions may also be achieved through an oxygen-associated insertion, and then a collapse or rearrangements of the unstable oxidized intermediate to provide various bond cleavage products, depending on the reaction conditions[2,7]. Such reactions suffer often from product variation as well as the problematic reaction selectivity. Other rare, non-selective C–C bond cleavages include those occurring in biotic,[21] photochemical,[22] or extreme[23] environments, and the controlled reactions taking place under metal- and oxidant-free conductions are still unprecedented.

Theoretically, the metal- and oxidant-free aromatic C–C bond cleavage are most likely to occur in bowl-shaped polycyclic aromatic hydrocarbon (PAH) systems[24,25], given that the intrinsic intramolecular strain and the less efficient π-delocalization for such non-planar structure are highly favourable driving force[26] for the cleavage. The strain energy of corannulene, the most notable example of the bowl-shaped PAHs, was estimated to be ca. 24.2 kcal mol^{-1},[27] which correlates with a large strain-release energy that would vigorously drive the bond scission.[28] The less efficient electron delocalization in the curved π-system of corannulene is anticipated to provide an additional driving force for C–C bond cleavage.[29] However, even for the bowl-shaped PAHs, C–C bond cleavages have been for a long time observed only under harsh experimental conditions, such as flash vacuum pyrolysis, laser annealing and electron impact ionization.[30–32].

Scheme 1. Cleavage of C–C bonds in corannulene systems.

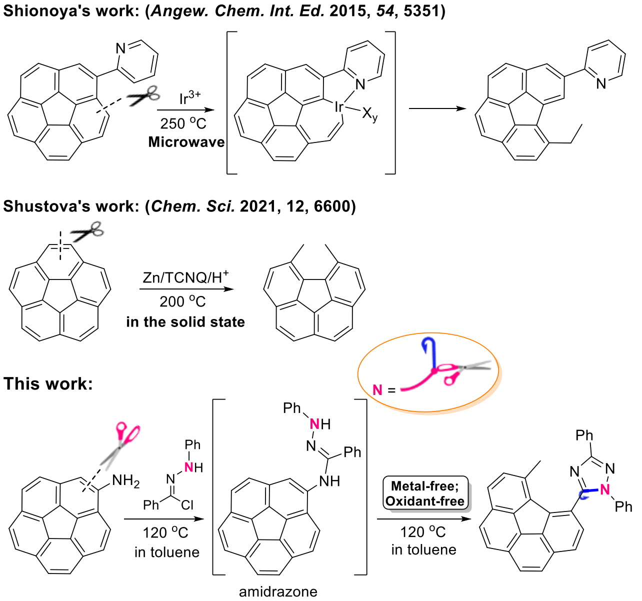

Recently, Shionoya *et al.*[33] described the first example of C−C bond cleavage in a corannulene derivative under microwave heating at 250 °C, for which the 2-pyridyl substituent was utilized as a directing group in the transition metal mediated reaction, to transform the curved corannulene skeleton to planar benzo[*ghi*]fluoranthene (Scheme 1). Shustova *et al.* recently reported the one-step C–C bond cleavage in corannulene in the solid state at 200 °C, using zinc

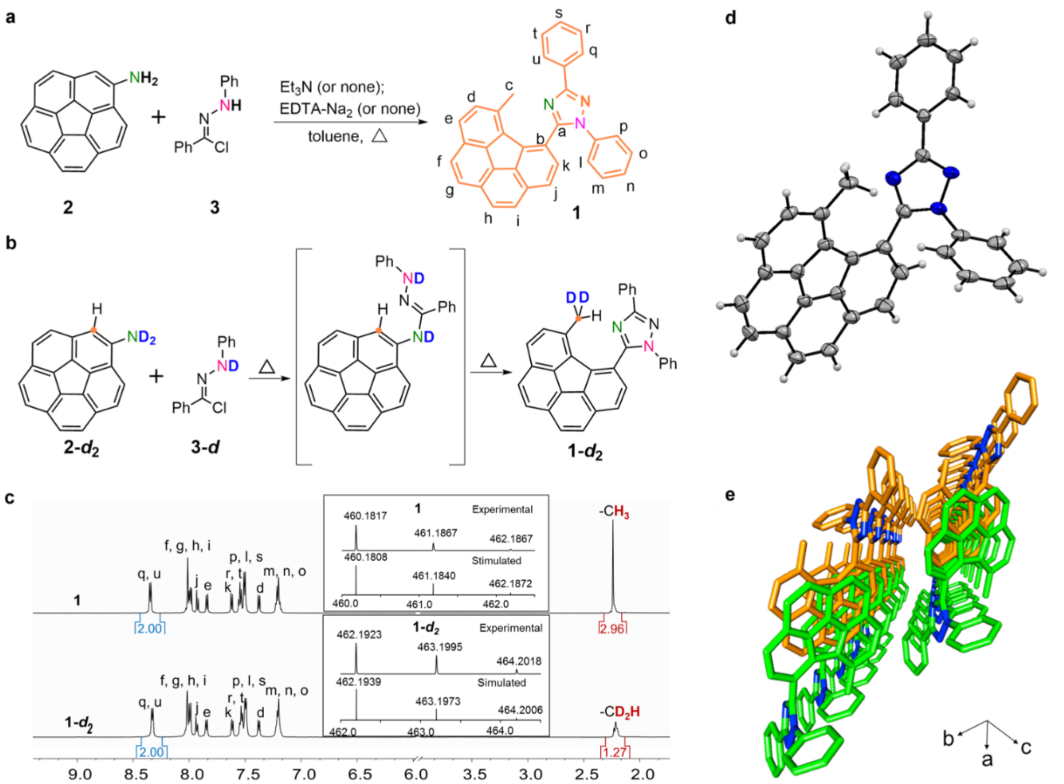

Figure 1. (a) The reaction of **2** and **3**. (b) The reaction of deuterated **2** and **3**, which gave the main product of **1-*d*₂**, along with small amounts of **1** and **1-*d***. Conditions: anhydrous toluene, 120 °C, 12 h. (c) ^{1}H NMR spectra (600 MHz, CD_2Cl_2, 298 K) of **1** and **1-*d*₂** (main fraction). The insets show the experimental and simulated isotopic clusters for **1** and **1-*d*₂**. Further details are reported in Figures S72–S75, SI. (d) X-ray molecular structure of **1**. (e) Paired packing of **1** into columns along a direction of slipped π−π stacking of benzo[*ghi*]fluoranthene moiety.

and a redox mediator in the presence of acid (Scheme 1).[34]

Herein, we report an aromatic C–C bond cleavage in corannulene under relatively mild, catalyst-free conditions, that effectively planarize the π-bowl structure to an “open” corannulene analog. The coupling of 1-aminocorannulene and hydrazonyl chloride offers a direct access to a 1,2,4-triazole-linked benzo[*ghi*]fluoranthene derivative (Scheme 1), manifesting the possibility of the controlled metal- and oxidant-free aromatic C–C bond cleavages.

Our initial objective of the studied reaction was to synthesize an amidrazone[35] to provide a π-extended Blatter radical according to the classical Neugebauer route.[36,37] However, we found that heating of 1-aminocorannulene (**2**) with *N*-phenylbenzenecarbohydrazonoyl chloride (**3**) (1:1 mol/mol) in the presence of base (Et_3N) provided **1** as an orange-yellow solid (Figure 1a). The yield of **1** increased with increasing reaction temperature, and in particular, the reaction carried out at 120°C for 12 h gave **1** in almost quantitative yield (Table S5, entries 4 – 6, Figures S1, S3 and S5, SI). We also found that the base Et_3N was not essential for the reaction (Table S5, entries 4 and 5, SI) and the presence of metal chelator (EDTA-Na_2) had no obvious influence on the product yield.

^{1}H NMR spectrum of **1** in [D_6]benzene showed distinct characteristic of the ring-opening products, in which the methyl moiety resulting from the C−C scission showed a well-resolved singlet at 2.20 ppm (Figure 1c). The corresponding ^{13}C NMR spectrum exhibited the methyl carbon signal at 21.1 ppm, which agreed well with the results of the DFT calculations (Table S8). The ESI-HRMS spectrum displayed an intense peak for $[\mathbf{1}+H]^{1+}$ at m/z = 460.1817 (Figure 1c), providing additional evidence for the generation of **1**.

The single crystal of **1** was successfully obtained by diffusion of cyclohexane into the solution of **1** in benzene at

Scheme 2. Control experiments. Anhydrous toluene was used as the solvent unless indicated otherwise. For details, see Part 3–5 and 7 in the SI.

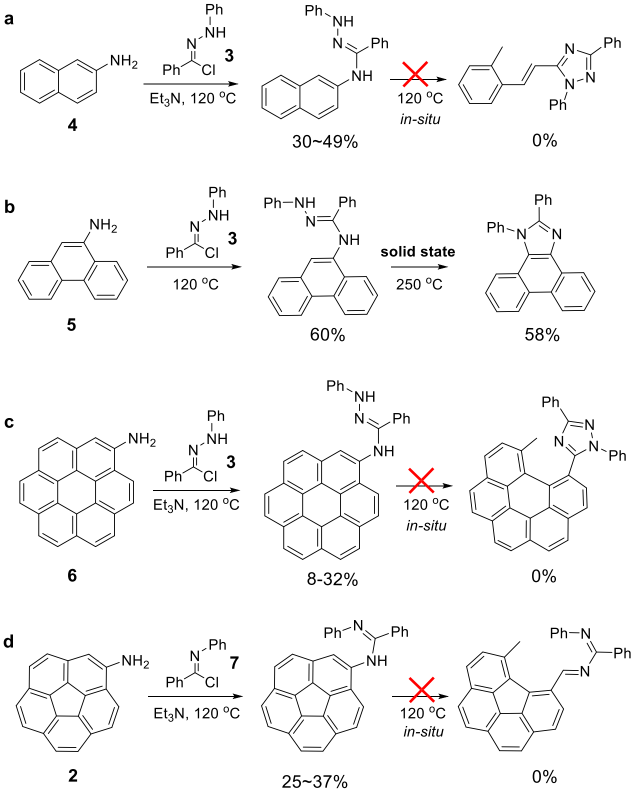

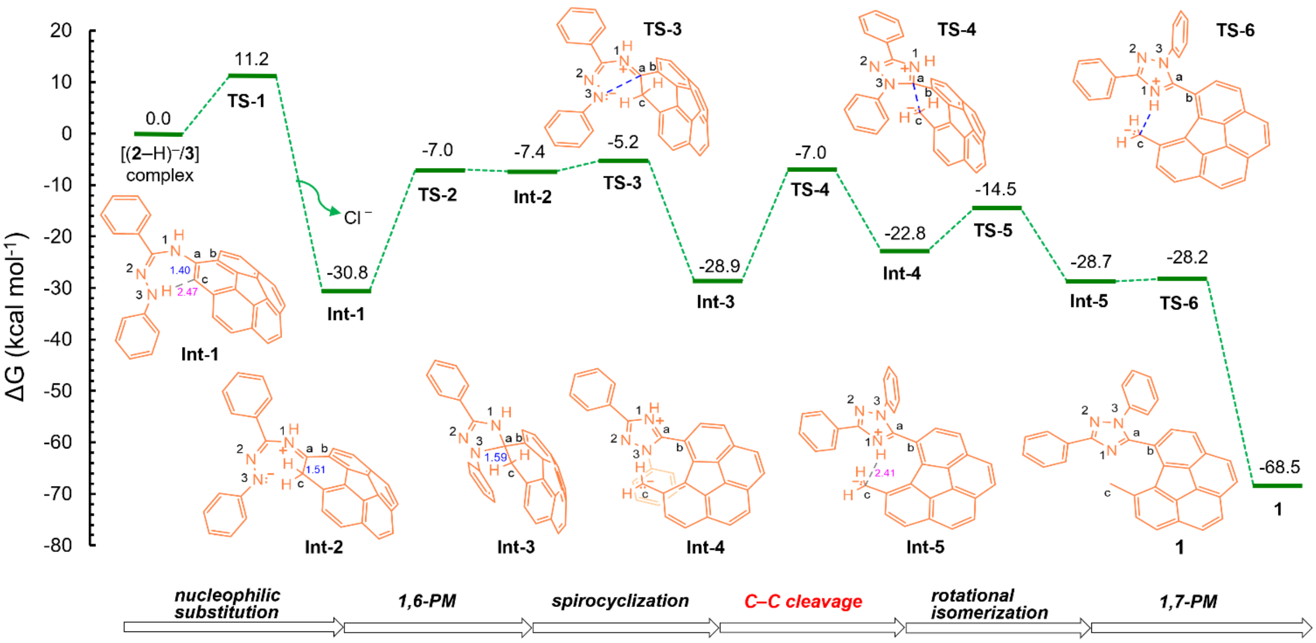

Figure 2. A DFT (B3LYP-D3BJ/6-31G(d)/PCM-UFF+ZPVE) calculated reaction pathway for the formation of **1** in benzene at 393 K. The C^a–C^c (blue numbers) and some (N)H–C^c (pink number) bond lengths are provided in Ångstroms.

ambient temperature. The X-ray structure of **1** showed a planar methyl substituted benzo[*ghi*]fluoranthene attached to a 1,3,5-trisubstituted 1,2,4-triazole, unambiguously confirming a C–C bond cleavage of the π-bowl to an "open" corannulene analog (Figure 1d). The solid-state packing of **1** is dominated by the slipped π-stacking[38] between equidistant planar benzo[*ghi*]fluoranthene moieties (Figure 1e) which is analogous to that in Shionoya's product.[33]

We carried out control reactions of amino-PAHs with various electrophiles, including **3**, to probe the effect of aromaticity and/or molecular strain on the reaction. Conveniently, the ^{1}H NMR spectral pattern of the putative product from the aromatic C–C bond cleavage should provide a readily observable signature signal at 2–3 ppm.

The reaction of planar aromatic amine, 2-naphthylamine (**4**) with **3** was first examined (Scheme 2a and Part 3, SI). The corresponding amidrazone was obtained in 30-49% yield. ^{1}H NMR spectra of the crude and the isolated products showed the absence of the signature signal at 2~3 ppm (Part 3, SI). Likewise, reacting 9-aminophenanthrene (**5**) with **3** gave the corresponding amidrazone. Heating the amidrazone in the solid state at 250 °C gave a phenanthro[9,10-*d*]imidazole in 58% yield (Scheme 2b and Part 4, SI) and the signature ^{1}H NMR signal was not detected. In addition, the reaction of 1-aminocoronene (**6**) and **3** produced the corresponding amidrazone in 8-32% yield without the observation of methyl ^{1}H NMR signal. (Scheme 2c and Part 5, SI). All these results suggested that the C–C cleavage in the reaction of **2** and **3** is likely driven by the strain energy of corannulene. Reacting **2** with (*Z*)–*N*–phenylbenzimidoyl chloride (**7**), which is an analog of **3** without an amine substituent at the imine nitrogen, afforded no products related to C–C bond cleavage (Scheme 2d and Part 7, SI). This indicates that the discovered aromatic C–C cleavage on corannulene was favourably facilitated by the ring annulation to 1,2,4-triazole moiety.

We speculated that the reaction pathway to **1**, via the ring annulation to 1,2,4-triazole and formation of methyl group, involves two intramolecular proton transfer processes. To verify this hypothesis, reaction of **2-*d*$_2$** and **3-*d*** was carried out (Figure 1b and Part 6, SI). As expected, the isolated product provided a very similar ^{1}H NMR spectrum as that of **1**, except the relative integration of the methyl group in the 2.0~2.2 ppm region was determined to be ~1.3 rather than 3.0 (Figure 1b). The predominant presence of **1-*d*$_2$** (with some **1-*d*** and **1**) is confirmed by the observation of ^{2}H–^{13}C couplings (Figure S74A–E) and isotopic upfield chemical shifts in the ^{1}H (Figure S72) and ^{13}C NMR spectra (Figure S74A–E), as well as by ESI HRMS analyses (Figure 1c and Figure S75A–D).

DFT (B3LYP-D3(BJ)/6-31G(d)) calculations, using solvent model for benzene (Gaussian 09 default),[39] are carried out to explore the C–C bond cleavage mechanism. Starting from the π-stacking complex of deprotonated **2** and **3**, the nucleophilic substitution provides the amidrazone **Int-1** via **TS-1,** with the Gibbs energy barrier of ~11.2 kcal mol^{-1} (Figure 2). An intramolecular 1,6-proton migration (1,6-PM) from the terminal anilino (N^3) group, located on the concave face of corannulene moiety, to carbon C^c in **Int-1**, provides **Int-2**. The C^a–C^c bond length in **Int-2** increases to 1.51 Å, compared to 1.40 Å in **Int-1**.

We should note that one of the corannulene 6-membered rings in **Int-2** loses its aromaticity to a large extent, as suggested by the absence of induced ring currents in AICD[40] plots and the small positive NICS(1)$_{zz}$[41] value (Figure S89).

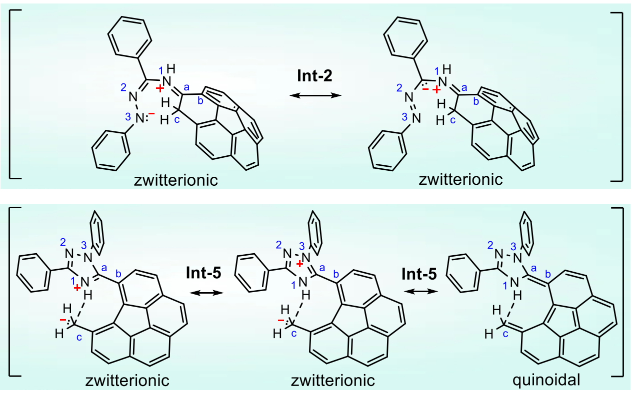

Figure 3. Zwitterionic/quinoidal resonance structures of **Int-2** and **Int-5**.

Furthermore, we view the structure of **Int-2** as an 1,5- or 1,3-zwitterion[42] stabilized by resonance (Figure 3). The subsequent collapse of the zwitterion, with the C–N bond formation between C^a and N^3, on the concave side of the PAH moiety, generates rapidly (energy barrier of only 2.2 kcal mol^{-1}) the spirocyclic intermediate **Int-3**.

The formation of spirocycle further increases the C^a–C^c bond length (1.59 Å). Ascribed to the weak C^a–C^c bond, the C^a–C^c cleavage corresponds to a remarkably low bond dissociation energy (ca. 6.1 kcal mol^{-1}), in contrast to that of 121 kcal mol^{-1} in benzene and 87 kcal mol^{-1} in cyclohexane.[43]

Rotation along the C^a–C^b bond in the sterically encumbered **Int-4** generates **Int-5** conformation that facilitates the N^1 to C^c intramolecular 1,7-proton migration (1,7-PM), leading to the formation of **1** (Figure 2). The intramolecular 1,7-proton migration has a very low activation barrier ($\Delta G^{\ddagger}_{393K}$ = 0.5 kcal mol^{-1}), due to the zwitterionic nature of both **Int-4** and **Int-5**, with some contribution of the quinoidal resonance form (Figure 3),[44] and the strong thermodynamic driving force (ca. 40 kcal mol^{-1} vs. **Int-5** or **Int-3**) to form **1** in the final step.

For the whole reaction process, thermodynamic relief of the strain energy appears to be the major factor in the C–C bond scission. We computed the reaction pathway for planar 1-aminocoronene (**6**) reacting with **3** to form a 1,2,4-triazole-linked benzo[*ghi*]perylene **Coron-Prd** (Figure S86). We found that the energy barriers of the first three steps are close to those of the analogous corannulene reaction (Figure S91). However, the C^a–C^c bond dissociation in spirocyclic intermediate **Coron-Int-3** (C^a–C^c bond length of 1.53 vs.1.59 Å in **Int-3**) requires a much higher energy than that in **Int-3** (36.2 *vs.* 6.1 kcal mol^{-1}). Correspondingly, the energy barrier for this rate-limiting step is as high as 43.5 kcal mol^{-1}, in contrast to that of only 21.9 kcal mol^{-1} in the case of corannulene. Also, the driving forces for the entire reaction sequence, which may be viewed as the Gibbs energy differences **1** vs. **Int-1** and **Coron-Prd** vs. **Coron-Int-1**, are -37.7 and -1.7 kcal mol^{-1}, respectively (Figure S91).

The formation of aromatic 1,2,4-triazole ring might provide an additional driving force for formation of **1**. Our computational results show that, starting from the corresponding spirocycle **Aliph-Int3**, to form an analogous product to **1** with a five-membered aliphatic ring, i.e., **Aliph-Prd**, the thermodynamic driving force is decreased by 18.0 kcal mol^{-1}, compared to the formation of **1** from **Int-3** (Figures S86 and S93).

DFT computed reaction pathway on the convex face of corannulene (Figure S87) indicates a similar energetics, from **Int-1** to **1**, to that on the concave face (Figure 2), thus suggesting that the formation of **1** may occur on either face of corannulene.

In summary, this work demonstrates the rare aromatic C–C bond cleavages occurred in a curved π-system of aminocorannulene under a metal- and oxidant-free conditions. The strain associated with the curved π-surface and the formation of aromatic triazole are the driving forces, among which the release of strain is the key point. The reaction pathway was facilitated by two intramolecular proton transfers and the formation of zwitterionic intermediates, leading to relatively low activation energies for the key steps. For the reaction, a weak basicity and moderately strong nucleophilicity of the –N^3– anion is crucial: too strong basicity and too weak nucleophilicity would hamper the 1,6-PM and the follow-up nucleophilic attack of the α-carbon (C^a in our studied case), respectively. Carbocationic character of the α-carbon is thus important. The results provide a better understanding of aromatic C–C cleavage and the disclosed reaction mechanism might be helpful to discover more reactions of this type in the future.

ASSOCIATED CONTENT

Data Availability Statement

The data underlying this study are available in the published article and its Supporting Information.

Supporting Information

The Supporting Information is available free of charge via the Internet at http://pubs.acs.org.

Detailed experimental procedures, characterization data, crystal data and DFT calculation results (PDF).

Accession Codes

CCDC 2087329, 2168617, and 2168622 contain the supplementary crystallographic data for this paper. These data can be obtained free of charge via www.ccdc.cam.ac.uk/data_request/cif, or by emailing data_request@ccdc.cam.ac.uk, or by contacting The Cambridge Crystallographic Data Centre, 12 Union Road, 495 Cambridge CB2 1EZ, UK; fax: +44 1223 336033.

AUTHOR INFORMATION

Corresponding Author

Ying Wang - College of Chemistry, Beijing Normal University, Beijing 100875, China; https://orcid.org/ 0000-0002-7015-7228; E-mail: ywang1@bnu.edu.cn
Andrzej Rajca - Department of Chemistry, University of Nebraska, Lincoln, Nebraska 68588-0304, United States; https://orcid.org/0000-0002-8856-1536; Email: arajca1@unl.edu
Hua Jiang - College of Chemistry, Beijing Normal University, Beijing 100875, China; https://orcid.org/ 0000-0002-9917-2683; Email: jiangh@bnu.edu.cn

Authors

Weijie Guo - College of Chemistry, Beijing Normal University, Beijing 100875, China.
Wanjian Ding - College of Chemistry, Beijing Normal University, Beijing 100875, China.
Yuqing Yao - College of Chemistry, Beijing Normal University, Beijing 100875, China.
Suchada Rajca - Department of Chemistry, University of Nebraska, Lincoln, Nebraska 68588-0304, United States.
Qiaolian Li - Institute of Chemistry, Chinese Academy of Sciences, Beijing 100190, China.

Author Contributions

$^+$W.G. and W.D. contributed equally to this work.

Notes

The authors declare no competing financial interest.

ACKNOWLEDGMENT

This work was supported by the National Science Foundation of China (21971021 and 21572023 to Y.W.; 21971020 to H.J.) and the National Science Foundation of the United States (CHE-1955349 and CHE-2247170 to A.R.).

REFERENCES

(1) Higashi, T.; Kusumoto, S; Nozaki, K. Cleavage of Si-H, B-H, and C-H Bonds by Metal-Ligand Cooperation. *Chem. Rev.*, **2019**, *119*, 10393−10402.

(2) Nairoukh, Z.; Cormier, M; Marek, I. Merging C–H and C–C bond cleavage in organic synthesis. *Nat. Rev. Chem.* **2017**, *1*, 0035.

(3) Wang, B.; Perea, M. A; Sarpong, R. Transition Metal-Mediated C–C Single Bond Cleavage: Making the Cut in Total Synthesis. *Angew. Chem. Int. Ed.* **2020**, *59*, 18898–18919.

(4) Shi, S-H.; Liang Y; Jiao N. Electrochemical Oxidation Induced Selective C−C Bond Cleavage. *Chem. Rev.* **2021**, *121*, 485−505.

(5) Jakoobi, M.; Sergeev, A. G., Transition-Metal-Mediated Cleavage of C-C Bonds in Aromatic Rings. *Chem. Asian .J* **2019,** *14*, 2181-2192.

(6) Chan, A. P. Y.; Sergeev, A. G., Metal-mediated cleavage of unsaturated C-C bonds. *Coord. Chem. Rev.* **2020,** *413*, 213213.

(7) Mandera, L. N.; Williams, C. M., Oxidative degradation of benzene rings. *Tetrahedron.* **2003**, *59*, 1105–1136.

(8) Lipscomb, J. D., Mechanism of extradiol aromatic ring-cleaving dioxygenases. *Curr. Opin. Struct. Biol.* **2008,** *18*, 644-649.

(9) Guengerich, F. P.; Yoshimoto, F. K., Formation and Cleavage of C-C Bonds by Enzymatic Oxidation-Reduction Reactions. *Chem. Rev.* **2018,** *118*, 6573-6655.

(10) Yan, K.; Yang, D.; Wei, W.; Li, G.; Sun, M.; Zhang, Q.; Tian, L.; Wang, H., Metal-free TBHP-mediated oxidative ring openings of 2-arylimidazopyridines via regioselective cleavage of C–C and C–N bonds. *RSC Adv.* **2015,** *5*, 100102-100105.

(11) Cai, Z.; Long, J.; Li, Y.; Ye, L.; Yin, B.; France, L. J.; Dong, J.; Zheng, L.; He, H.; Liu, S.; Tsang, S. C. E.; Li, X., Selective Production of Diethyl Maleate via Oxidative Cleavage of Lignin Aromatic Unit. *Chem* **2019,** *5*, 2365-2377.

(12) Fliszár, S.; Cardinal, G.; Baykara, N. A. Charge distributions and chemical effects. XL. Chemical bonds in benzenoid hydrocarbons. *Can. J. Chem.* **1986**, *64*, 404.

(13) Jakoobi, M.; Halcovitch, N.; Whitehead, G. F.; Sergeev, A. G., Selective Arene Cleavage by Direct Insertion of Iridium into the Aromatic Ring. *Angew. Chem. Int. Ed.* **2017,** *56*, 3266-3269.

(14) Jakoobi, M.; Tian, Y.; Boulatov, R.; Sergeev, A. G., Reversible Insertion of Ir into Arene Ring C-C Bonds with Improved Regioselectivity at a Higher Reaction Temperature. *J. Am. Chem. Soc.* **2019,** *141*, 6048-6053.

(15) Hicks, J.; Vasko, P.; Goicoechea, J. M.; Aldridge, S. Reversible, Room-Temperature C-C Bond Activation of Benzene by an Isolable Metal Complex. *J. Am. Chem. Soc.* **2019,** *141*, 11000-11003.

(16) Qiu, X.; Sang, Y.; Wu, H.; Xue, X-S.; Yan, Z.; Wang, Y.; Cheng, Z.; Wang, X.; Tan, H.; Song, S.; Zhang, G.; Zhang, X.; Houk, K. N.; Jiao, N. Cleaving arene rings for acyclic alkenylnitrile synthesis. *Nature* **2021**, *597*, 64–69.

(17) Szyszko, B.; Latos-Grażyński, L.; Szterenberg, L., A Facile Palladium-Mediated Contraction of Benzene to Cyclopentadiene: Transformations of Palladium(II) p-Benziporphyrin. *Angew. Chem. Int. Ed.* **2011,** *50*, 6587-6591.

(18) Hurej, K.; Pawlicki, M.; Szterenberg, L.; Latos-Grażyński, L., A Rhodium-Mediated Contraction of Benzene to Cyclopentadiene: Transformations of Rhodium(III) *m*-Benziporphyrin. *Angew. Chem. Int. Ed.* **2016,** *55*, 1427-1431.

(19) Kang, X.; Luo, G.; Luo, L.; Hu, S.; Luo, Y.; Hou, Z., Mechanistic Insights into Ring Cleavage and Contraction of Benzene over a Titanium Hydride Cluster. *J. Am. Chem. Soc.* **2016,** *138*, 11550-11559.

(20) Ford, A.; Miel, H.; Ring, A.; Slattery, C. N.; Maguire, A. R.; McKervey, M. A., Modern Organic Synthesis with alpha-Diazocarbonyl Compounds. *Chem. Rev.* **2015,** *115*, 9981-10080.

(21) Field, J. A.; Sierra-Alvarez, R., Microbial degradation of chlorinated benzenes. *Biodegradation* **2008,** *19*, 463-80.

(22) Modanlu, S.; Shafiekhani, A., Synthesis of pure and C/S/N co-doped Titania on Al mesh and their photocatalytic usage in Benzene degradation. *Sci. Rep.* **2019,** *9*, 16648.

(23) Betowski, L. D.; Winnik, W.; Marcus, A. B.; Pyle, S. M., The nature of $C_{10}H_2^+$ in mass spectra of polynuclear aromatic hydrocarbons. *Int. J. Mass Spectrom. Ion Process.* **1998**, *173*, 27–39.

(24) Wu, Y.-T.; Siegel, J. S., Aromatic Molecular-Bowl Hydrocarbons: Synthetic Derivatives, Their Structures, and Physical Properties. *Chem. Rev.* **2006**, *106*, 4843−4867.

(25) Tsefrikas, V. M.; Scott, L. T., Geodesic Polyarenes by Flash Vacuum Pyrolysis. *Chem. Rev.* **2006**, *106*, 4868−4884.

(26) Zhou, Z.; Kawade, R. K.; Wei, Z.; Kuriakose, F.; Üngör, Ö.; Jo, M.; Shatruk, M.; Gershoni-Poranne, R.; Petrukhina, M. A.; Alabugin, I. V., Negative Charge as a Lens for Concentrating Antiaromaticity: Using a Pentagonal "Defect" and Helicene Strain for Cyclizations. *Angew. Chem. Int. Ed.,* **2020**, *59*, 1256-1262.

(27) Sun, C. H.; Lu, G. Q.; Cheng, H. M., Nonplanar Distortions and Strain Energies of Polycyclic Aromatic Hydrocarbons. *J. Phys. Chem. B* **2006**, *110*, 4563-4568.

(28) Fumagalli, G.; Stanton, S.; Bower, J. F., Recent Methodologies That Exploit C-C Single-Bond Cleavage of Strained Ring Systems by Transition Metal Complexes. *Chem Rev* **2017,** *117*, 9404-9432.

(29) Dobrowolski, M. A.; Ciesielski, A.; Cyranski, M. K., On the aromatic stabilization of corannulene and coronene. *Phys. Chem. Chem. Phys.* **2011,** *13*, 20557-20563.

(30) Attar, S.; Forkey, D. M.; Olmstead, M. M.; Balch, A. L.; Crystallographic characterization of the helical diketone, $C_{36}H_{14}O_2$, a new product from the flash vacuum pyrolysis of decacyclene in the presence of oxygen. *Chem. Commun.* **1998**, 1255–1256.

(31) Inada, Y.; Amaya, T.; Shimizu, Y.; Saeki, A.; Otsuka, T.; Tsuji, R.; Seki, S.; Hirao, T., Nitrogen-doped Graphitic Carbon Synthesized by Laser Annealing of Sumanenemonoone Imine as a Bowl-shaped p-Conjugated Molecule. *Chem. Asian J.* **2013,** *8*, 2569-2674.

(32) Wang, X.; Becker, H.; Hopkinson, A. C.; March, R. E.; Scott, L. T.; Bçhme, D. K., Collision-induced dissociation of 2- and 3-dimensional polycyclic aromatic hydrocarbon cations in a modified ion-trap detector. *Int. J. Mass Spectrom. Ion Processes* **1997**, *161*, 69–76.

(33) Tashiro, S.; Yamada, M.; Shionoya, M., Iridium-catalyzed reductive carbon-carbon bond cleavage reaction on a curved pyridyl-corannulene skeleton. *Angew. Chem. Int. Ed.* **2015,** *54*, 5351-5354.

(34) Leith, G. A.; Rice, A. M.; Yarbrough, B. J.; Kittikhunnatham, P.; Mathur, A.; Morris, N. A.; Francis, M. J.; Berseneva, A. A.; Dhull, P.; Adams, R. D.; Bobo, M. V.; Vannucci, A. A.; Smith, M. D.; Garashchuk, S.; Shustova, N. B., "Broken-hearted" carbon bowl via electron shuttle reaction: energetics and electron coupling. *Chem. Sci.* **2021,** *12*, 6600-6606.

(35) Al-Noaimi, M.; AlDamen, M. A., Ruthenium complexes incorporating azoimine and α-diamine based ligands: Synthesis, crystal structure, electrochemistry and DFT calculation. *Inorganica Chim. Acta,* **2012,** *387*, 45-51.

(36) Neugebauer, F. A.; Umminger, I., Über 1,4-Dihydro-l,2,4-benzotriazinyl-Radikal. *Chem. Ber.* **1980**, *113*, 1205−1225.

(37) Cicculo, F.; Gallagher, N. M.; Geladari, O.; Chasse, T.; Rajca, A.; Casu, M. B., A Derivative of the Blatter Radical as a Potential Metal-Free Magnet for Stable Thin Films and Interfaces. *ACS Appl. Mater. Interfaces.* **2016,** *8*, 1805-1812.

(38) Yao, Z.-F.; Wang, J.-Y.; Pei, J., Control of π–π Stacking via Crystal Engineering in Organic Conjugated Small Molecule Crystals. *Cryst. Growth Des.* **2017,** *18*, 7-15.

(39) M. J. Frisch,; G. W. Trucks,; H. B. Schlegel,; et al. Gaussian 09, revision D.01; Gaussian, Inc.: Wallingford, CT, 2013.

(40) Geuenich, D.; Hess, K.; Köhler, F.; Herges, R., Anisotropy of the Induced Current Density (ACID), a General Method To Quantify and Visualize Electronic Delocalization. *Chem. Rev.* **2005**, *105*, 3758−3772.

(41) Chen, Z.; Wannere, C. S.; Corminboeuf, C.; Puchta, R.; P. v. R. Schleyer., Nucleus-Independent Chemical Shifts (NICS) as an Aromaticity Criterion. *Chem. Rev.*, **2005**, *105*, 3842−3888.

(42) Alternatively, **Int-2** might be viewed as a diradical. However, broken symmetry UB3LYP-D3(BJ)/6-31G(d,p) computaions in benzene, as outlined in the SI, indicate that the singlet diradicaloid character is negligible.

(43) Exner, K.; Schleyer, P. R., *J. Phys. Chem. A.* **2001**, *105*, 3407–3416.

(44) Contribution of quinoidal resonance form, with a C^a–C^b double bond, to conformations **Int-4** and **Int-5** is relatively small as illustrated by the interconversion barriers of only about 8 and 14 kcal mol^{-1}.